Resonant-optical-second-harmonic generation from thin C_{60} films

Bert Koopmans, Anton Anema, Harry T. Jonkman, George A. Sawatzky, and Folkert van der Woude
Laboratory of Solid State Physics, Materials Science Centre, University of Groningen, Nijenborgh 4, 9747 AG Groningen, The Netherlands
(Received 22 July 1992)

We studied the optical-second-harmonic generation from thin C_{60} films, using a combination of frequency-, rotational-, angular-, and film-thickness-dependent measurements. We present a method to resolve the phase of $\chi^{(2)}$ by exploiting the interference between the C_{60} overlayer contribution and the anisotropic Si(111) substrate contributions. We find a strong and sharp resonance at $2\hbar\omega = 3.60$ eV. The linewidth is found to be surprisingly small as compared to linear ellipsometry and third-harmonic-generation experiments. The intensity as a function of film thickness agrees with a model considering interference effects between equal second-harmonic contributions from the inner C_{60}/Si interface and the outer C_{60} surface. The possibility of nonlocal bulk contributions is discussed.

I. INTRODUCTION

Soon after the discovery of C_{60} and other C_{2n} fullerenes,[1,2] speculation started about possible large nonlinear optical (NLO) properties. The strong NLO response of the fullerenes is an interesting feature in itself In addition, second-order optical techniques yield information about the local surface and interface electronic structure of thin fullerene films. During the past decade there has been a growing interest of this application of second-harmonic generation (SHG) and sum frequency generation.[3,4] Due to the inherent interface sensitivity, these techniques are even applicable to buried interfaces.[5]

Recently, high cubic polarizabilities have been reported for C_{60} and C_{70}, obtained from third-harmonic generation[6,7] (THG) and degenerate four-wave-mixing[8] experiments at infrared fundamental frequencies ($\hbar\omega = 0.5$ to 1.2 eV). The large hyperpolarizabilities of the fullerenes are a result of the strong delocalization of the conjugated π-electronic structure as in the conjugated hydrocarbons. Since the most common fullerene molecules C_{60} and C_{70} posses inversion symmetry (point groups I_h and D_{5h}), second-order NLO processes are forbidden within the dipole approximation. High second-order polarizabilities can be obtained by forming charge-transfer complexes of the symmetric fullerenes.[6] However, solid fullerenes also show quite large SH effects, as already shown for 1.17-eV radiation.[9,10] This second-order response can be explained either by C_{60} surface and C_{60}/substrate interface dipole-allowed processes or by nonlocal (electric quadrupole and magnetic dipole) bulk effects. Due to the large size of the C_{60} molecule, and the large delocalization length of the important electronic eigenstates, the bulk contributions might be of particular importance. In this paper we describe detailed experiments on pure C_{60} thin films, to our knowledge the first spectroscopic SHG study of pure C_{60} films or C_{60} surfaces. We indeed found the C_{60} films to show a high SHG efficiency, and strong resonant features at $2\hbar\omega$ close to an allowed optical transition. The results are compared with linear ellipsometry,[11] and frequency-resolved THG experiments.[7]

Specific phase-sensitive second-harmonic (SH) experiments can provide information about the full complex behavior of the SH susceptibility tensor $\chi^{(2)}$.[12–14] Such phase measurements are of particular interest in nonlinear optics, since in general the frequency regions available in NLO do not allow a reliable Kramers-Kronig transformation. In this paper we present a method which is applicable to thin-film geometries. The phase information is resolved from the interference of different symmetry SH contributions from the thin film and its substrate, as obtained from rotational anisotropic SHG experiments. For these experiments we used slightly stepped Si(111) substrates because of their well-known anisotropic response, and the additional anisotropic contribution caused by the steps.

To compare the surface and interface electronic structure, we performed *in situ* SHG measurements as function of the film thickness. Differences of $\chi^{(2)}$ from the outer surface and the inner interface are resolved using the interference between the two contributions. However, the separation of surface-interface and bulk contributions is not trivial, as discussed in several papers.[15,16] In an ordinary reflection or transmission experiment the only nonzero nonlocal bulk contribution $\gamma\nabla(\mathbf{E}\cdot\mathbf{E})$ is easily shown to be inseparable from a certain combination of surface susceptibility components. Within the thin-film geometry as used by us a second nonzero bulk contribution is present: $\delta'(\mathbf{E}\cdot\nabla)\mathbf{E}$, which *is* separable. The experiments as shown in this paper do not yet resolve these bulk contributions, but include the bulk effects as effective interface-surface contributions. However, from preliminary experiments we know that bulk as well as surface-interface contributions are of importance. In principle, the techniques as presented here can be used to study a variety of thin-film systems, though in practice the combination of optical parameters of the system may limit the full applicability of the techniques.

II. EXPERIMENT

C_{60} with a purity better than 99.99% was obtained from Syncom BV. A Knudsen cell was used to evaporate thin films of C_{60} onto hydrogen-terminated Si(111) single crystals, which were kept at 200 °C during evaporation. For optimal use in the rotational SHG experiments the Si surfaces where slightly stepped with a misorientation of 4° and steps normal to the (11$\underline{2}$) direction. All preparation and optical experiments were carried out in an ultrahigh-vacuum (UHV) chamber with a base pressure of 5×10^{-10} mbar. During evaporation the pressure was kept below 2×10^{-9} mbar. The layer thickness was calibrated from the interference as observed in a linear reflection experiment. After etching and rinsing of the Si substrates outside the vacuum, we did not expose them to any cleaning procedures inside the UHV. However careful checks showed the SH signals of the Si substrate to be stable for periods of several days inside the UHV, which validates its use as a reference source.

For the SH experiments a dye laser was pumped by a Nd:YAG (yttrium aluminum garnet) laser, producing 5-ns pulses with frequencies in the range $\hbar\omega=1.6$ to 2.0 eV. SH intensities were calibrated by the use of a reference quartz crystal in transmission geometry, carefully tuned to a Maker fringe optimum by fine tuning the frequency. Corrections were made for the variable coherence length in the crystal as a function of the photon energy. Throughout this paper, SH efficiencies are represented by the SH reflection coefficient $R_{SH}=I_{SH}/I_0^2$, where I_0 is the incident intensity and I_{SH} is the intensity at the double frequency. The absolute size of the complex SH amplitudes are defined as the square root of the corresponding SH reflection coefficient, which allows easy conversion between efficiencies and amplitudes.

Rotational and angular scans were performed by using a specially developed UHV compatible goniometer. The setup enables full 360° scans, rotating the sample about its surface normal, as well as continuous scans (0° to ±80°) over the angle of incidence. *In situ* layer-thickness-dependent SH experiments have been carried out during evaporation at a fixed rotation of the sample and a fixed angle of incidence (45°).

III. RESULTS AND DISCUSSION

A. Rotational anisotropy

The stepped Si(111) substrates generate a rotational anisotropic SH signal.[17] Steps normal to the (11$\underline{2}$) direction lower the surface symmetry from C_{3v} [as for a pure (111) surface] to C_{1v}. The resulting SH intensity I_{SH} as a function of the rotation angle ψ can be written generally as

$$I_{SH}(\psi)=|A_0+A_1\cos(\psi)+A_3\cos(3\psi)|^2 . \quad (1)$$

The SH signal has contributions with three different rotational symmetries: Isotropic with complex amplitude $A_0=a_0e^{i\phi_0}$, onefold $A_1=a_1e^{i\phi_1}$ (due to the steps) and threefold $A_3=a_3e^{i\phi_3}$ (due to the terraces, bulk contributions, and overtones of the step contributions). The actual values of the amplitudes depend on the reflection angle and on the polarization combination of the incident and the reflected beam. The experiments as presented in this paper are carried out within a $p\rightarrow p$ geometry and at a 45° angle of incidence. Under these conditions all three contributions are present, and for a misorientation of approximately 4° within the same order of magnitude for the bare substrate.

Because in ordinary SH experiments only the intensity is measured, the absolute phase information of $\chi^{(2)}$ is lost. However, if one deals with a superposition of contributions exhibiting different rotational symmetries, it is easily seen that the relative phase information between the different contributions is retained, e.g., $\phi_1-\phi_0$ and $\phi_3-\phi_0$ in Eq. (1). This motivates our choice of substrates with a well-defined symmetry, even if the overlayer turns out to yield only isotropic response. Moreover the overlayer might adapt the anisotropy of the substrate, though this has not been observed in the present experiments.

The evolution of the various complex amplitudes during stepwise evaporation of additional C_{60} is shown in Fig. 1. The SH frequency ($2\hbar\omega=3.54$ eV) is chosen close to a SH resonance as will be shown in Sec. III C. From the figure one learns that within fair approximation amplitudes a_1 and a_3, as well as the relative phases, are independent of the presence and thickness of a C_{60} overlayer. On the other hand, the isotropic contribution is strongly enhanced by increasing the layer thickness. These observations validate a model of an overlayer which is electronically completely decoupled from the

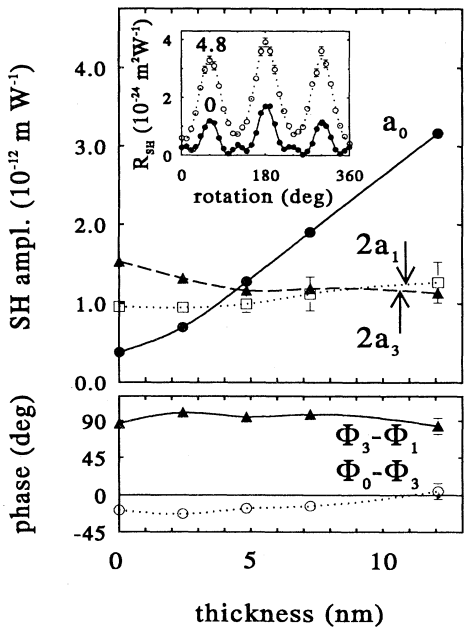

FIG. 1. The separate rotational symmetry contributions of C_{60} films of various film thicknesses, as measured at $2\hbar\omega=3.54$ eV. The data points are obtained from least-square fits of Eq. (1) to rotational SHG patterns, as shown in the inset for the bare substrate (●) and 4.8-nm C_{60} (○). The top section shows the amplitudes a_0 (●), a_1 (□), and a_3 (▲); the bottom section shows the relative phases $\phi_0-\phi_3$ (○) and $\phi_3-\phi_1$ (▲). The curves are meant to guide the eye.

substrate, at least as far as SHG is concerned. As a consequence, $\chi^{(2)}$ of the total system can be described by the sum of $\chi^{(2)}$ of the bare substrate and $\chi^{(2)}$ of the overlayer.

Figure 1 also shows that the C_{60} overlayer gives rise to merely isotropic SHG. The continuous increase of the isotropic intensity far beyond 2 monolayers (1 monolayer corresponds to approximately 1 nm) might seem an unexpected result, especially in light of former studies on various overlayers on metals, where SH intensities saturate after evaporation of a few monolayers.[18] This continued increase is investigated by means of *in situ* thickness scans, where the SH intensity is measured continuously up to much higher thickness.

B. Thickness dependence

Figure 2 shows a thickness scan, also performed at $2\hbar\omega=3.54$ eV and at fixed rotation $\psi=90°$. At this specific rotation the onefold and threefold contributions vanish, and on the scale of Fig. 2 the isotropic contribution of the bare substrate is negligible. The scan shows a very pronounced thickness (t) dependence. The oscillation at high thickness has been found to proceed in an almost undamped manner up to at least 2000 nm. The period of this high thickness oscillation is equivalent to the linear reflection period.

For not too thin films we can explain the interference pattern accurately with a three-layer model (0=vacuum, 1=C_{60}, 2=substrate), and with surface SH susceptibilities assigned to both interfaces; $\chi_s^{(2)}$ for the outer surface at $z=0$, and $\chi_i^{(2)}$ for the inner interface at $z=-t$, where the z axis is perpendicular to the interfaces. Although not included explicitly, the bulk contributions γ and δ' can be incorporated in $\chi_s^{(2)}$ and $\chi_i^{(2)}$ for this fixed $p\rightarrow p$ polarized experiment.[19] In defining the optical parameters we make use of small symbols at the fundamental frequency and capitals at the SH frequency: λ (Λ) is the wavelength in vacuum; n_i (N_i), k_i (K_i), and θ_i (Θ_i) are the refractive index, the extinction coefficient, and the propagation angle relative to the surface normal in medium i, respectively; and $r_{ij}(R_{ij})$ and t_{ij} (T_{ij}) are the Fresnel reflection and transmission coefficients from medium i to j, for p-polarized light. A value of $n_1=1.98$ (Ref. 11) at $\hbar\omega=1.77$ eV is used for the thickness calibration, where one full period corresponds to $\Delta t=\lambda/(2n_1\cos\theta_1)$. We note that the thin C_{60} film is almost transparent at ω (i.e., $k_1\ll\lambda/t$) but strongly absorbing at 2ω.

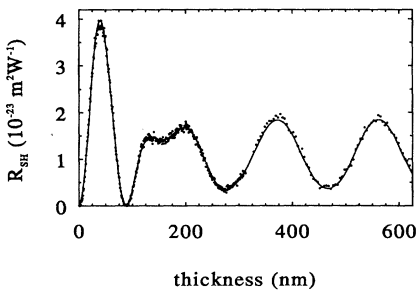

FIG. 2. The isotropic SH efficiency $R_{SH}=I_{SH}/I_0^2$ as measured during evaporation of C_{60} at $2\hbar\omega=3.54$ eV and at a fixed rotation angle $\psi=90°$. The solid curve represents a least-squares fit of Eqs. (2)–(4), neglecting tensor components other than $\chi^{(2)}_{zzz}$. The reflection coefficients are fixed consistent with Refs. 11 and 20, except for r_{12}, as explained in the text. This yields a ratio of $\chi_i^{(2)}/\chi_s^{(2)}=-1.03e^{2^{\circ}i}$ close to -1.

There are two interfering contributions to the total SH signal: (1) The interface contribution is driven by the local field at the interface, and is damped out exponentially due to absorption in the film of the generated SH radiation. (2) The surface contribution is driven by the local field at the surface, which is the sum of the incoming and interface-reflected fields, and therefore shows the same interference period as found in a linear reflection experiment. At high thickness beyond 300 nm, only this surface SHG contributes. The observed low intensity at very thin film thickness can be explained by a dominant quadrupole bulk contribution, but also by destructively interfering true (dipolar) surface and interface SH contributions. The latter situation would be an indication for weak electronic interactions between the overlayer and the substrate, in which case the outer surface and the inner interface of the C_{60} are characterized by approximately opposite SH susceptibilities ($\chi_i^{(2)}\approx-\chi_s^{(2)}$). This weak bonding is consistent with the use of saturated Si substrates.

To define a proper theoretical model, we follow the convention as described by Mizrahi and Sipe:[16] The driving fields for the SHG are measured just within the C_{60} at $z=0^-$ and $z=-t^-$. At the outer surface, the induced SH radiation source is taken in the vacuum just outside C_{60}, at $z=0^+$. At the interface we introduce an infinitely thin vacuum gap at $z=-t$ between the C_{60} and the substrate, and place the SH radiation source within this gap. Then one can derive for the total SH intensity for the three-layer model as function of film thickness:

$$I_{SH}(t)=\frac{32\pi^3\omega^2}{c^3\cos^2\theta_0}|(A_s+A_i)|^2I_0^2\ , \tag{2}$$

where surface and interface contributions (A_s and A_i) can be written by introducing the normalized thicknesses $d=(2\pi t/\lambda)(n_1-ik_1)\cos\theta_1$ and $D=(2\pi t/\Lambda)(N_1-iK_1)\cos\Theta_1$,

$$A_s(t)=\sum_{\mu,\nu,\xi}t_{01}^2(1+s_\mu R_{01})\frac{(1+s_\mu R_{12}e^{-2iD})}{(1-R_{10}R_{12}e^{-2iD})}\times\frac{(1+s_\nu r_{12}e^{-2id})(1+s_\xi r_{12}e^{-2id})}{(1-r_{10}r_{12}e^{-2id})^2}\times F_\mu f_\nu f_\xi\chi^{(2)}_{s,\mu\nu\xi}\ , \tag{3}$$

$$A_i(t)=\sum_{\mu,\nu,\xi}t_{01}^2(1+s_\mu R_{01})\frac{(1+s_\mu R_{12})e^{-iD}}{(1-R_{10}R_{12}e^{-2iD})}\times\frac{(1+s_\nu r_{12})(1+s_\xi r_{12})e^{-2id}}{(1-r_{10}r_{12}e^{-2id})^2}\times F_\mu f_\nu f_\xi\chi^{(2)}_{i,\mu\nu\xi}\ , \tag{4}$$

where $\mu,\nu,\xi \in \{\|,z\}$ and $\|$ components are parallel to the surface and for a $p \rightarrow p$ geometry in the plane of incidence. We defined the projection factors $F_z = \sin\Theta_0$, $F_\| = \cos\Theta_0$, $f_z = \sin\theta_1$, and $f_\| = \cos\theta_1$, and the factors $s_z = -s_\| = 1$. For the isotropic SHG from C_{60}, the only nonvanishing tensor components are $\chi^{(2)}_{zzz}$, $\chi^{(2)}_{z\|\|}$, and $\chi^{(2)}_{\|z\|} = \chi^{(2)}_{\|\|z}$. The factors s_z and $s_\|$ account for the fact that the perpendicular and parallel components of reflected fields are given by R_{ij} and $-R_{ij}$, respectively. A least-squares fit using $\chi^{(2)}_{zzz}$ components only, and a straightforward substitution of reflection coefficients according to the refractive indices as found in Refs. 11 and 20, already gives a very good agreement. However, to account for small deviations due to the other tensor components, we also fit the value of r_{12}. This results in $(r_{12})_{\text{eff}} = 0.258e^{-8°i}$, slightly less than the $r_{12} = 0.288e^{0.1°i}$ from the literature. Apart from an overall scaling factor, there are only two adjustable parameters in the model: the ratio $\chi^{(2)}_i/\chi^{(2)}_s$ and r_{12}. We find a ratio $\chi^{(2)}_i/\chi^{(2)}_s = -1.03e^{2°i}$, approximately equal to -1 indeed. Although the $\chi^{(2)}_{z\|\|}$ and $\chi^{(2)}_{\|z\|}$ components can not be obtained uniquely from this single experiment, we estimate these components to be one to two orders of magnitude smaller than the $\chi^{(2)}_{zzz}$ components, as obtained from a fit with r_{12} fixed to its appropriate value.

Concerning the strength of the SH effects we conclude that C_{60} really has a high surface SH efficiency; at the first interference maximum $R_{\text{SH}} \sim 4\times10^{-23}$ $\text{m}^2\,\text{W}^{-1}$. This is even large compared to SHG from the most efficient free-electron-like metallic surfaces [e.g., Al at $\theta_0 = 75°$: $R \sim 2\times10^{-23}$ $\text{m}^2\,\text{W}^{-1}$ (Ref. 21)]. As discussed before, the large $\chi^{(2)}$ is a result of large delocalization of the relevant molecular electronic states. Complete explicit separation into bulk and surface-interface contributions is not possible from the present experiment. Only the deviation of $\chi^{(2)}_i/\chi^{(2)}_s$ from minus unity, as well as possible minor $\chi^{(2)}_{\|z\|}$ contributions can be shown to be true surface and interface effects. Here we would like to point out that the method as used by Wang *et al.* to separate the surface and bulk contributions from their transmission SHG experiments[9] is only partly correct. They correctly suggest that the SH contribution in the limit of zero thickness must be a surface contribution (in fact, the difference of surface and interface contributions), but incorrectly assign bulk character to all the remaining thickness dependent part. Their "bulk" contribution can equally well be described by opposite surface and interface susceptibilities.

So far we neglected finite-thickness effects of the film. However, for very thin films the proposed model might break down, e.g., due to direct coupling at 2ω between the radiating polarization sheets at $z = 0^+$ and $z = -t$. For films thinner than two monolayers the presented model collapses definitely, because the concept of two separated radiating sheets is no longer valid. In that case microscopic details such as the distribution of C_{60} across the surface have to be considered.

C. Frequency dependence

In order to study phase-resolved resonant effects, the frequency dependence of the rotational SHG patterns for

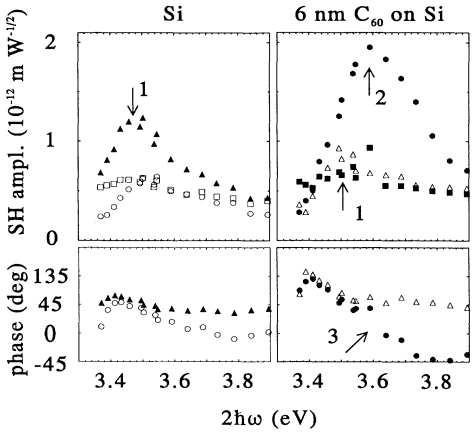

FIG. 3. Dispersion of the different SH contributions for a bare Si substrate (left) and a 6-nm C_{60} film (right). Top panels: SH amplitudes a_0 (○,●), a_1 (□,■), and a_3 (▲,△). Bottom panels: SH phases $\phi_0 - \phi_1$ (○,●) and $\phi_3 - \phi_1$ (▲,△). The arrows indicate some special features: the weak Si resonance in a_0 and a_3 ("1"), and the enhanced a_0 ("2") and rapid phase change of $\phi_0 - \phi_1$ ("3") accompanying the C_{60} resonance.

bare substrates and for thin (5–10 nm) C_{60} layers has been thoroughly analyzed in the frequency range $2\hbar\omega = 3.2$ to 4 eV. Each rotational pattern offers a set of amplitudes and relative phases as shown in Fig. 3 for a C_{60} film of 6-nm thickness. The isotropic and threefold amplitudes of bare Si show a small resonant feature around $2\hbar\omega = 3.4$–3.5 eV. This resonance is absent in the onefold contribution. The resonance can be explained by the E_1 peak at 3.4 eV in the imaginary part of the bulk dielectric constant of Si,[20] which explains its absence in the pure surface onefold contribution. The absence of resonant features suggest the onefold susceptibility components to have a constant phase and to be predominantly of real character ($\phi_1 \approx 0°$). This provides the possibility of an absolute phase calibration by relating the phase of the isotropic and threefold contribution to ϕ_1.

We concluded from Fig. 1 that the C_{60} SHG is decoupled from the substrate SHG. This holds approximately at all frequencies of Fig. 3. Using this conclusion in combination with the assumption of a constant $\phi_1 \approx 0$, we obtain pure C_{60} SH susceptibility by subtracting the isotropic $A_0 = a_0 e^{i(\phi_0 - \phi_1)}$ of the bare Si substrate from A_0 of the evaporated C_{60} data. The resulting difference spectrum is shown in Fig. 4. A clear resonant structure is found, which can be well reproduced by a single Lorentzian superimposed onto a dispersionless real background. This yields for the isotropic SH amplitude of the isolated film:

$$A_{\text{SH}}(-2\omega;\omega,\omega) = \left[\frac{a_{\text{res}}}{2\omega - \omega_0 - i\Gamma} + a_0\right] e^{-i\phi_1}; \qquad (5)$$

ω_0 and Γ are the resonance frequency and linewidth of a particular electronic transition, a_{res} is proportional to the oscillator strength, and the nondispersive a_0 could be ap-

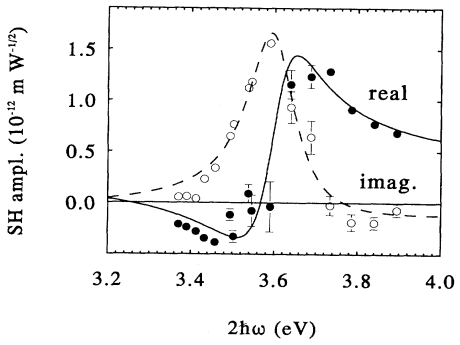

FIG. 4. The phase-resolved dispersion of the pure C_{60} SH amplitudes as obtained by subtracting the isotropic amplitude $A_0 = a_0 e^{i(\phi_0 - \phi_1)}$ of the bare substrate from A_0 of the C_{60}/Si system, and assuming a constant $\phi_1 (\approx 0)$. The drawn curves represent the real (full line) and imaginary (dotted) part of a fit of Eq. (5) with parameters: $\omega_0 = 3.60 \pm 0.01$ eV, $\Gamma = 0.07 \pm 0.01$ eV, and a resonant enhancement $a_{res}/(\Gamma a_0) = 5.6$.

proximately equal to the low-frequency amplitude as measured by the infrared experiments. We explicitly include a prefactor $e^{i\phi_1}$ in order to account for a possible nonzero phase of the onefold Si contribution. The fit as shown in Fig. 4 is obtained with $\phi_1 = 0$. This seems to be a proper assumption, since the out-of-phase contribution shows a maximum just at resonance. The slightly negative imaginary part at higher frequencies might indicate a ϕ_1 somewhat different from zero. Unlike the linear case however, a negative imaginary second-order susceptibility is not strictly forbidden.

As shown in Eq. (5) we expect the observed SH resonance to be a result of electronic transitions at $2\hbar\omega$. With this interpretation $\hbar\omega_0 = 3.60$ eV is very close to one of the $A_g \rightarrow T_{1u}$ transition found, e.g., in ellipsometry at 3.56 eV.[11] One may doubt the significance of this small shift. Nevertheless, the direction is consistent with a reduction of the screening of the T_{1u} excitation at the surface, and may be compared to the shift between solid C_{60} and C_{60} in a n-hexane solution (3.56 → 3.78 eV).[22]

It is striking that the SH linewidth $\Gamma = 0.07$ eV is three times smaller than the linewidth as found in ellipsometry: $\Gamma = 0.23$ eV. Also resonant THG experiments have been reported, showing only broad features. The THG resonance at $3\hbar\omega = 2.8$ eV closely resembles the linear absorption profile.[7] This discrepancy between the SHG linewidth and the linear-THG linewidth might be related to the inherent interface and surface sensitivity of the second-order process, i.e., relate to specific properties of interface and surface electronic states. However, recent experiments seem to indicate the significance of bulk contributions to the SHG process. Although an intriguing question, so far we did not find any conclusive explanation for this narrow linewidth.

Finally we note that even better fits can be obtained if one allows for slightly different resonance parameters for surface, bulk, and interface. Such differences could be expected physically because of the different environment, which also shows up in the ratio $\chi_i^{(2)}/\chi_s^{(2)}$ slightly differing from -1. However at present, due to the statistics and probably also the number of necessary data manipulations, a unique resolution of those differences is not possible. Furthermore, inhomogeneous non-Lorentzian line broadening may also modify the line shape and therefore complicate the explicit separation into surface, bulk, and interface resonances.

IV. CONCLUSIONS

Using various SH interference techniques as described in this paper we studied the SH response of thin C_{60} films. Complicated interference patterns as function of film thickness, could be reproduced well by a simple two sheet model. Rotational anisotropic SHG measurements were used to resolve the real and the imaginary part of the SH susceptibility tensor. For the C_{60} films we were able to fully map the sharp resonance at $2\hbar\omega = 3.60$ eV. Its remarkable narrow linewidth is still an outstanding question. Although we found evidence for at least some surface and interface contributions, a complete separation into surface, bulk, and interface contributions is impossible from the described experiments. Present experiments using different combinations of polarization geometry, as well as angle of incidence-dependent experiments will be more conclusive in this respect.

Preliminary results of experiments as we recently carried out for C_{60} on Cu substrates show quite distinct results. We find a significantly enhanced SH interface contribution from C_{60} on properly cleaned substrates as compared to oxidized substrates, which may be explained by charge transfer between the C_{60} and the substrate, thus enhancing the local dipole fields at the interface. Comparable phenomena might be found for clean (flash heated) Si surfaces, where the presence of highly reactive dangling Si bonds could give rise to chemiabsorption of the C_{60} molecules. SHG techniques as presented in this paper will be a very sensitive probe for these chemisorption-induced structural and spectral changes at the interface.

ACKNOWLEDGMENTS

This investigation was supported by the Netherlands Foundation for Fundamental Research on Matter (FOM) with financial support from the Netherlands Organization for the Advancement of Pure Research (NWO).

[1] H. W. Kroto, J. R. Heath, S. C. O'Brien, R. F. Curl, and R. E. Smalley, Nature **318**, 162 (1985).
[2] W. Krätschmer, L. D. Lamb, K. Fostiropoulos, and D. R. Huffman, Nature **347**, 354 (1990).
[3] Y. R. Shen, Annu. Rev. Phys. Chem. **40**, 327 (1989).
[4] G. L. Richmond, J. M. Robinson, and V. L. Shannon, Prog. Surf. Sci. **28**, 1 (1988).
[5] T. F. Heinz, F. J. Himpsel, E. Palange, and E. Burstein, Phys.

Rev. Lett. **63**, 644 (1989).
[6]Y. Wang, and L.-T. Cheng, J. Phys. Chem. **96**, 1530 (1992).
[7]J. S. Meth, H. Vanherzeele, and Y. Wang, Chem. Phys. Lett. **197**, 26 (1992).
[8]W. J. Blau, H. J. Byrne, D. J. Cardin, T. J. Dennis, J. P. Hare, H. W. Kroto, R. Taylor, and D. R. M. Walton, Phys. Rev. Lett. **67**, 1423 (1991). *The reported values of γ and some of the interpretation has been questioned by Ref. 9;* R. J. Knize and J. P. Partanen, *ibid.* **68**, 2704 (1992); Z. H. Kafafi, F. J. Bartoli, J. R. Lindle, and R. G. S. Pong, *ibid.* **68**, 2705 (1992).
[9]X. K. Wang, T. G. Zhang, W. P. Lin, S. Z. Liu, G. K. Wong, M. M. Kappes, R. P. H. Chang, and J. B. Ketterson, Appl. Phys. Lett. **60**, 810 (1992).
[10]H. Hoshi, N. Nakamura, Y. Maruyama, T. Nakagawa, S. Suzuki, H. Shiromaur, and Y. Achiba, Jpn. J. Appl. Phys. **30**, L1397 (1991).
[11]S. L. Ren, Y. Wang, A. M. Rao, E. McRae, J. M. Holden, T. Hager, K. Wang, W. T. Lee, H. F. Ni, J. Selegue, and P. C. Ecklund, Appl. Phys. Lett. **59**, 2678 (1991).
[12]R. K. Chang, J. Ducuing, and N. Bleombergen, Phys. Rev. Lett. **15**, 6 (1965).
[13]K. Kemnitz, K. Bhattacharyya, J. M. Hicks, G. R. Pinto, K. B. Eisenthal, and T. F. Heinz, Chem. Phys. Lett. **131**, 285 (1986).
[14]G. Berkovic, Y. R. Shen, G. Marowsky, and R. Steinhoff, J. Opt. Soc. Am. B **6**, 205 (1989).
[15]J. E. Sipe, V. Mizrahi, and G. I. Stegeman, Phys. Rev. B **35**, 9091 (1987).
[16]V. Mizrahi and J. E. Sipe, J. Opt. Soc. Am B **5**, 660 (1988).
[17]C. W. van Hasselt, M. A. Verheijen, and Th. Rasing, Phys. Rev. B **42**, 9263 (1990).
[18]H. W. K. Tom, C. M. Mate, X. D. Zhu, J. E. Crowell, T. F. Heinz, G. A. Somorjai, and Y. R. Shen, Phys. Rev. Lett. **52**, 348 (1948); H. W. K. Tom, C. M. Mate, X. D. Zhu, J. E. Crowell, Y. R. Shen, and G. A. Somorjai, Surf. Sci. **172**, 466 (1986).
[19]B. Koopmans, A. M. Janner, H. T. Jonkman, G. A. Sawatzky, and F. van der Woude (unpublished).
[20]D. E. Aspnes and A. A. Studna, Phys. Rev. B **27**, 985 (1983).
[21]R. Murphy, M. Yeganeh, K. J. Song, and E. W. Plummer, Phys. Rev. Lett. **63**, 318 (1989).
[22]S. Leach, M. Vervloet, A. Desprès, E. Bréheret, J. P. Hare, T. J. Dennis, H. W. Kroto, R. Taylor, and D. R. M. Walton, Chem. Phys. **160**, 451 (1992).